Suppression of the Polarization Bremsstrahlung from a Fast Charged Particle in an Amorphous Medium

V. A. Astapenko[a],* and N. N. Nasonov[b]

[a] *Moscow Institute of Physics and Technology, Institutskiĭ per. 9, Dolgoprudnyĭ, Moscow oblast, 141700 Russia*

[b] *Belgorod State University, Studencheskaya ul. 14, Belgorod, 308007 Russia*

* *e-mail: astval@mail.ru*

Abstract—Based on a consistent quantum-mechanical approach, we calculate and analyze the suppression of the polarization bremsstrahlung (PB) from a fast charged particle moving in an amorphous medium. The suppression effect is attributable to destructive interference between the contributions from atoms of condensed material to the bremsstrahlung due to their finite sizes and chaotic arrangement. We calculate the spectral and angular PB dependences on various targets that demonstrate characteristic features of the phenomenon under consideration. We have established the region of the clearest manifestation of the suppression effect. The results obtained by various methods of calculation are compared.

1. INTRODUCTION

Polarization bremsstrahlung (PB) is an additional (to the traditional mechanism) channel of bremsstrahlung from charged particles scattered by atoms in a medium that arises from the conversion of the intrinsic field of an incident particle into a real photon on target electrons [1–3]. Just as in the traditional (Bethe–Heitler) mechanism, the PB energy is drawn from the kinetic energy of a radiating charge. The essential difference between the Bethe–Heitler and polarization bremsstrahlung mechanisms is that the polarization channel is not directly related to the incident particle acceleration. This determines the characteristic features of the polarization mechanism, in particular, the independence of the PB intensity from the radiating-particle mass. In addition, in contrast to the Bethe–Heitler channel, the polarization bremsstrahlung of fast particles is produced far from the nuclei of target atoms, so one might expect a manifestation of significant cooperative effects in PB at high atomic density. Such effects in radiative processes have also been investigated previously. For example, the classical electrodynamic effects of transition radiation [4] or parametric X-ray radiation [5–8] are determined by the coherent (in contribution from target atoms) PB component [9], i.e., they are collective radiative processes.

Since the spectral and angular PB parameters depend on the mutual arrangement of atoms in a target, we can count on a method being developed for diagnosing the atomic structure of a material based on the measurement of these parameters. Experimental measurements of the spectra of the collimated PB from relativistic electrons in polycrystalline samples of various elements have shown a high sensitivity of the PB properties to the structure of the materials under study [10, 11].

In this paper, we investigate the cooperative effects that arise in PB when charges are scattered in an amorphous material. The interference between the contributions from various atoms to the X-ray scattering in a dense amorphous medium is known to be destructive in nature [12]. Destructiveness also manifests itself during the conversion of the intrinsic field of an incident particle into a real photon in such a medium. In general, this causes the bremsstrahlung intensity to decrease. The possibility of this kind of suppression of the polarization channel was first pointed out in [13], where PB was calculated by means of classical electrodynamics. The effect of PB suppression when a relativistic electron is scattered in amorphous carbon was detected in an experiment [14].

In [13], the numerical results were obtained in the high-frequency approximation for the response of atoms in the medium to the perturbation produced by the field of an incident particle. This approximation is valid only for high bremsstrahlung photon energies. At the same time, the suppression effect under consideration is significant precisely in the low-frequency part of the spectrum. Thus, there is a need for quantitatively describing the cooperative effects in PB in an amorphous medium on the basis of a consistent approach that takes into account the dynamics of target electrons over the entire range of frequencies, emission angles, and incident particle energies. This description is important, because the PB suppression must be taken into account when interpreting the results of PB mea-

surements whose goal is the above diagnostics of the atomic structure of materials.

2. THE PB INTENSITY IN AN AMORPHOUS MEDIUM

As we noted in the Introduction, the polarization bremsstrahlung mechanism can be described as the scattering of the virtual photon of the intrinsic field of an incident particle into a real photon. According to this interpretation, the following expression can be derived for the PB amplitude of a relativistic charged particle on the jth atom of the medium by the standard quantum-mechanical method [1, Ch. 5] (the atomic units $\hbar = e = m_e = 1$ are used everywhere):

$$T_j = 2\pi i\delta(\omega + (\mathbf{q}-\mathbf{k})\cdot\mathbf{v})\sqrt{\frac{2\pi}{\omega}}\frac{1}{\tilde{c}}[\mathbf{s}\cdot\mathbf{A}^{(p)}(q)] \times \omega^2\alpha(\omega,\mathbf{q})\exp(i\mathbf{q}\cdot\mathbf{r}_j), \quad \mathbf{q} = \mathbf{p}_f - \mathbf{p}_i + \mathbf{k}. \tag{1}$$

Here, $\tilde{c} = c/n(\omega)$ is the phase velocity of light in the medium, $n(\omega)$ is the refractive index, ω and $\mathbf{k}$ are the frequency and wave vector of the emitted photon, $\mathbf{p}_{i,f}$ are the initial and final momenta of the incident particle, $\mathbf{s}$ is a unit vector in the direction of photon emission, $\mathbf{r}_j$ is the radius vector of the atomic nucleus, $\alpha(\omega, \mathbf{q})$ is the dynamic polarizability of the atom, and $\mathbf{A}^{(p)}(q)$ is the vector potential of the electromagnetic field of the scattered charge:

$$\mathbf{A}^{(p)}(q) = \frac{4\pi\tilde{c}Z_p}{\omega}\frac{\omega\mathbf{v}/\tilde{c}^2 + (\mathbf{q}-\mathbf{k})}{(\omega/\tilde{c})^2 - (\mathbf{q}-\mathbf{k})^2}, \tag{2}$$

where $\mathbf{v}$ and Z_p are the velocity and charge of the incident particle, respectively. Equation (1) was derived in the first Born approximation in incident particle–target electron interaction. This is valid for fast particles, which we assume below. In deriving Eq. (1), we performed summation over the radiation polarizations and assumed that the state of the atom during the virtual photon scattering did not change. The substitution $c \longrightarrow \tilde{c}$ reflects the renormalization of the photon propagator as a result of the zero-angle electromagnetic-field scattering by electrons of the medium [1, Ch. 6], so the photon scattering that leads to the propagator renormalization is elastic in nature. In this way, it differs fundamentally from the scattering responsible for PB, which requires the transfer of energy–momentum excess to the target. Thus, the above types of electromagnetic-field scattering in a material are physically separated; therefore, they may be taken into account independently when calculating the PB intensity.

After the summation of partial amplitudes (1) over the atoms in a unit volume and the integration over the momentum transferred to the medium, we obtain the following expression for the differential PB intensity normalized to the atomic density:

$$\frac{dI_{\text{amor}}}{d\omega d\Omega_{\mathbf{s}}} = \int_{q_{\min}}^{q_{\max}} T_{\text{amor}}(q)dq, \qquad q_{\min}(\omega, v, \theta) = \frac{\omega}{v}\left(1 - \frac{v}{\tilde{c}}\cos\theta\right), \quad q_{\max} = 2\mu v, \tag{3}$$

where $T(q)$ is the partial PB intensity in an amorphous material normalized to the atomic density N, $d\Omega_{\mathbf{s}}$ is the solid angle in the direction of photon emission, $\theta = \widehat{\mathbf{p}_i\mathbf{k}}$ is the emission angle of the bremsstrahlung photon, and μ is the reduced mass of the incident particle and the electron. The partial PB intensity is given by the formula [15]

$$T_{\text{amor}}(q) = \frac{2Z_p^2}{\pi\tilde{c}^3 vq}S_{\text{amor}}(q)|Z_{\text{pol}}(\omega, q)|^2 I\phi(q, v, \omega, \theta), \tag{4}$$

where $Z_{\text{pol}}(\omega, q) = \omega^2|\alpha(\omega, q)|$ is the effective polarization charge of the atoms in the medium and $I\phi(q, v, \omega, \theta)$ is the dimensionless integral defined by the equality

$$I\phi(q, v, \omega, \theta) = \frac{q^3 v}{2\pi} \times \int d\Omega_{\mathbf{q}}\delta(\omega - \mathbf{k}\cdot\mathbf{v} + \mathbf{q}\cdot\mathbf{v})\frac{[\mathbf{s}, \omega\mathbf{v}/\tilde{c}^2 - \mathbf{q}]^2}{(\mathbf{q}^2 - 2\mathbf{k}\cdot\mathbf{q})^2}. \tag{5}$$

After cumbersome algebraic transformations, integral (5) can be represented as a function of three variables,

$$I\phi(q, v, \omega, \theta) = \tilde{I}\phi(x = q/(\omega/\tilde{c}), \beta = v/\tilde{c}, \theta),$$

where

$$\tilde{I}\phi(x, \beta, \theta) = \frac{x^2 f_1(x, \beta, \theta)}{\Delta^{3/2}(x, \beta, \theta)} + \frac{x^2}{4}\left[\frac{f_2(x, \beta, \theta)}{\Delta^{1/2}(x, \beta, \theta)} - 1\right], \tag{6}$$

$$f_1 = (x^2 + 2x_{\min}\cos\theta) \times [(x^2 - x_{\min}^2)\cos^2\theta + (x_{\min} - \beta)^2\sin^2\theta] + 4(x_{\min} - \beta)(x^2 - x_{\min}^2)\sin^2\theta\cos\theta, \tag{7}$$

$$f_2 = x^2 + 2x_{\min}\cos\theta, \qquad x_{\min} = \frac{\tilde{c}q_{\min}}{\omega} = \beta^{-1} - \cos\theta, \tag{8}$$

$$\Delta = \left(x^2 - 2\left(1 - \frac{\cos\theta}{\beta}\right)\right)^2 + 4\frac{1-\beta^2}{\beta^2}\sin^2\theta. \tag{9}$$

In the relativistic limit ($\beta \longrightarrow 1$), the function $\tilde{I}\phi(x, \beta, \theta)$ has a sharp maximum when

$$x^{(m)} = \sqrt{2(1-\cos\theta/\beta)} \approx 2\sin(\theta/2),$$

the sharpness of the maximum increases for large emission angles $\theta \longrightarrow \pi$. At the maximum, the following approximate equality can be obtained using Eqs. (7)–(9):

$$\tilde{I}\phi(x^{(m)}) \approx \tilde{\gamma}\frac{\tan(\theta/2)}{2},$$

where

$$\tilde{\gamma} \approx \frac{\gamma}{\sqrt{1+\gamma^2(1-\varepsilon(\omega))}}$$

(we assume that $\varepsilon(\omega) < 1$). Hence follows the density effect in PB [16], which manifests itself as a decrease in the bremsstrahlung intensity if $\gamma^2(1-\varepsilon(\omega)) > 1$.

The function $S(\mathbf{q})$ in Eq. (4) is the normalized structure factor of the material defined by

$$\begin{aligned} S(\mathbf{q}) &= N^{-1}\sum_{j,l}\langle\exp(i\mathbf{q}\cdot(\mathbf{r}_j-\mathbf{r}_l))\rangle \\ &= 1+N\int[g(r)-1]\exp(i\mathbf{q}\cdot\mathbf{r})d\mathbf{r}. \end{aligned} \tag{10}$$

The second equality in Eq. (10), where $g(r)$ is the pair correlation function of the atoms, applies to an isotropic medium. For the structure factor of an amorphous material in the hard-sphere approximation, where $g(r) = \Theta(r-d)$ (d is the mean atomic diameter and $\Theta(x)$ is the theta function), it follows from Eq. (10) (see [12]) that

$$S_{\text{amor}}(q) = \left[1-\sigma\frac{3j_1(qd)}{qd}\right], \quad \sigma = \frac{4\pi N d^3}{3}, \tag{11}$$

where $j_1(x)$ is the spherical Bessel function of the first order. The second term in the square brackets of the first equality in Eq. (10) reflects the destructive interference between the contributions from atoms of the amorphous medium to the total PB intensity. Clearly, the PB suppression effect related to this interference is significant in the case where the parameter σ is close to unity. In addition, for this effect to manifest itself, the argument of the spherical Bessel function $x = qd$ must be smaller than unity. Hence, using the expression for the minimum momentum transferred to the medium $q_{\min}$ (the second equality in (3)), we obtain

$$\omega < \frac{v}{d(1-(v/\tilde{c})\cos\theta)}. \tag{12}$$

This inequality (when $\sigma \approx 1$) defines the spectral range of PB suppression in an amorphous medium as a function of the incident particle velocity and the photon emission angle. Such parameters of the problem at which the contribution from low transferred momenta (large impact parameters) to the process is significant correspond to the physical condition (12). PB is then collective in nature; the various atoms are mutually screened, thereby reducing the intensity of the process. This screening can be interpreted just as the destructive interference between the elementary PB fields produced by individual atoms.

To characterize the influence of cooperative effects on PB in an amorphous material, it is convenient to introduce the bremsstrahlung suppression ratio

$$K = \frac{dI_{\text{amor}}}{dI_{\text{at}}},$$

where dI_{at} is the differential PB intensity on an isolated atom. The expression for the atomic PB intensity follows from Eqs. (3) and (4) if we set $S_{\text{amor}} = 1$ and $\tilde{c} = c$ in Eq. (4). In the hard-sphere approximation (11), the K factor is

$$\begin{aligned} &K(\omega, v, \theta) \\ &= \frac{\displaystyle\int_{q_{\min}}^{q_{\max}}\left(1-\sigma\frac{3j_1(qd)}{qd}\right)\alpha(\omega, q)I\phi(q, v, \omega, \theta, \tilde{c})\frac{dq}{q}}{\displaystyle\int_{q_{\min}}^{q_{\max}}\alpha(\omega, q)I\phi(q, v, \omega, \theta, c)\frac{dq}{q}}. \end{aligned} \tag{13}$$

If low transferred momenta such that $q < d^{-1}$ make a major contribution to the PB intensity, then a simple estimate for the suppression ratio follows from Eq. (13): with a logarithmic accuracy,

$$K \approx 1-\sigma.$$

This estimate was obtained in [13] in the low-frequency limit $\omega \longrightarrow 0$ (in this case, it should be kept in mind that the approach [13] is inapplicable in the limit under consideration). In particular, it follows from this estimate that a necessary condition for the adequacy of the model under consideration is the inequality $\sigma \le 1$.

Using the hard-sphere approximation (11) to calculate the PB intensity requires knowing the parameter

$$\sigma = 4\pi N d^3/3.$$

Whereas the atomic density can be easily estimated from the known density of the material, difficulties can arise in determining the mean atomic radius d, which is a model quantity, particularly in the case of a medium with a high atomic density. As an example, let us illustrate the aforesaid for the structure factor of liquid silicon, for which the results of quantum-chemical calcu-

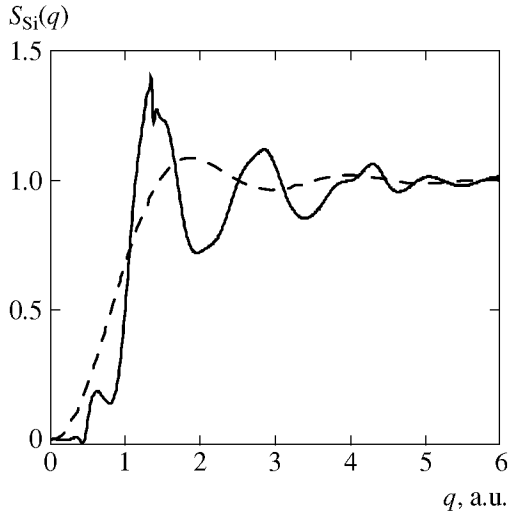

Fig. 1. Structure factor of liquid silicon: the quantum-chemical calculation [17] (solid curve) and the hard-sphere approximation (11) for $\sigma = 1$ (dashed curve).

lations are presented in [17]. The dependence of the structure factor on the momentum q transferred to the medium at the silicon melting temperature $T = 1410°C$ calculated in [17] is shown in Fig. 1. Also shown in this figure is the structure factor of liquid silicon calculated in the hard-sphere model for $\sigma = 1$. This value of σ for the actual liquid silicon density $N = 5.446 \times 10^{22}$ cm^{-3} corresponds to the mean atomic diameter $d = 1.64$ Å, which was used to construct the dashed curve in Fig. 1. At the same time, the tabulated diameter of the silicon atom is $d = 2.36$ Å [18]. (Note that twice the Wigner–Seitz radius for the above density of silicon atoms is 3.27 Å). However, $\sigma \approx 3$ at this value of d, so $S(q \longrightarrow 0) < 0$, which is in conflict with the positive definiteness of the structure factor of the medium.

A similar conclusion can be reached for amorphous carbon and other condensed media of light atoms where the model structure factor (11) causes a conflict with the numerical values of the parameters of the problem. Note that the pair correlation function $g(r)$ used in [17] to determine $S(q)$ differs markedly from the theta function of the hard-sphere model. This difference is particularly great at small distances, $r \approx d$, where the correlation function has a maximum: $g \approx 2$. The latter suggests the presence of a short-range order in liquid silicon at its melting temperature.

As follows from Eq. (4), to calculate the PB intensity, we must know the explicit form of the function

$$Z_{pol}(\omega, q) = \omega^2 |\alpha(\omega, q)|$$

and $\mathrm{Re}\,\alpha(\omega)$ (to calculate $\tilde{c}$). Below, we will use the following approximation for the generalized dynamic polarizability of the atom:

$$\alpha(\omega, q) \approx \alpha(\omega) F(q), \qquad (14)$$

where $\alpha(\omega)$ is the dipole polarizability and $F(q)$ is the atomic form factor normalized as $F(0) = 1$. Approximation (14) can be justified using consistent quantum-mechanical calculations in terms of the random phase approximation with exchange [3]. To obtain the frequency dependence of the imaginary part of the dipole polarizability, we will proceed from its relation to the photoabsorption cross section $\sigma_{ph}(\omega)$ given by the optical theorem:

$$\mathrm{Im}(\alpha(\omega)) = \frac{c}{4\pi\omega}\sigma_{ph}(\omega). \qquad (15)$$

In this paper, we use the data on the photoabsorption coefficient given at the website of the National Institute of Standards and Technology [19] to determine the spectral dependence $\sigma_{ph}(\omega)$. The real part of the atomic polarizability can be restored from the known imaginary part using the Kramers–Kronig relation, which is useful to represent as

$$\mathrm{Re}(\alpha(\omega)) = \frac{2}{\pi}\int_0^\infty \frac{\omega\,\mathrm{Im}(\alpha(\omega)) - \omega'\mathrm{Im}(\alpha(\omega'))}{\omega^2 - \omega'^2} d\omega'. \qquad (16)$$

Equation (16) allows the principal-value integral appearing in the standard form of the Kramers–Kronig relation to be calculated via an integral with the removed point that eliminates the singularity of the integrand, which is convenient in practical calculations.

Comparison of the complex polarizability calculated using Eqs. (15) and (16) with the data obtained in the random phase approximation with exchange shows [3] that the relative discrepancy between the results does not exceed 10% over a wide frequency range.

In the high-frequency limit, the polarization charge is equal to the number of bound electrons in the atom, since $\alpha(\omega) = -Z/\omega^2$ (Z is the nuclear charge equal to the number of bound electrons) in this case. Our calculation shows that the polarizability reaches the high-frequency asymptotics in the case of a silicon atom for photon energies above 2 keV. At $\omega < 200$ eV, the high-frequency approximation strongly distorts the actual picture. The first extremum in the frequency dependence of the polarization silicon charge corresponds to the excitation energy of the $L_{2,3}(2p)$ subshell (104 eV); the last (indistinct) extremum corresponds to the excitation of the K shell (1844 eV) [20].

The frequency dependence of the refractive index for liquid silicon,

$$n(\omega) = \sqrt{1 + 4\pi N \mathrm{Re}\,\alpha(\omega)},$$

was calculated using Eqs. (15) and (16) for the atomic density $N = 5.446 \times 10^{22}$ cm^{-3}. The refractive index differs markedly from unity at photon energies $\omega <$ 500 eV; at $\omega > 125$ eV, the refractive index is less than unity. Our analysis shows that in the case under consid-

eration, the refractive index calculated in the high-frequency approximation adequately describes the actual situation at photon energies $\omega > 200$ eV. For lower photon energies, the high-frequency model strongly distorts the actual picture. It is important to emphasize that the refractive index of the medium in the high-frequency approximation is always less than unity, so this approximation is qualitatively incapable of describing effects like the Cherenkov radiation.

To calculate the atomic form factor $F(q)$, which defines the dependence of the generalized atomic polarizability on the transferred momentum in approximation (14), it is convenient to use the Slater wave functions of atomic orbitals. As was shown in [21], the form factor calculated in this way differs from its Hartree–Fock analog by no more than a few percent. The corresponding formulas are

$$F(q) = \frac{1}{Z}\sum_j N_j Q(q, \beta_j, \mu_j),$$

$$Q(q, \beta, \mu) = \frac{[1 + (q/2\beta)^2]^{\mu}}{\mu q/\beta} \times \sin\left[2\mu \arctan\left(\frac{q}{2\beta}\right)\right], \quad (17)$$

where N_j is the number of equivalent electrons in the jth atomic shell, β and μ are the Slater parameters of the atomic orbitals.

3. NUMERICAL RESULTS AND DISCUSSION

Let us use the formulas derived in the previous section to calculate the spectral and angular dependences of the PB intensity for a fast electron scattered in an amorphous medium. Let is first consider the process on a bulk sample of liquid silicon, for which quantum-chemical calculations of the structure factor are available [17]. Figure 2 presents the spectral PB intensities in liquid silicon normalized to the density of the medium and for the electron scattering by an isolated atom. The plots in Fig. 2 were constructed for a relativistic electron with a Lorentz factor of $\gamma = 10$ at a bremsstrahlung photon emission angle of $\theta = 18°$. The maximum in the spectral dependence for an isolated atom is attributable to an increase in the polarization charge of the silicon atom when the bremsstrahlung photon energy approaches the K-shell energy. We see that the PB intensity in liquid silicon is considerably lower than that in the single-atom case over the entire range of photon energies due to the destructive interference between the contributions from various atoms discussed above. Our calculation show that for a larger emission angle, $\theta = 90°$, and the same remaining parameters, PB suppression takes place in the low-energy range $\omega < 3$ keV. This corresponds to inequality (12), which defines the domain of existence of the

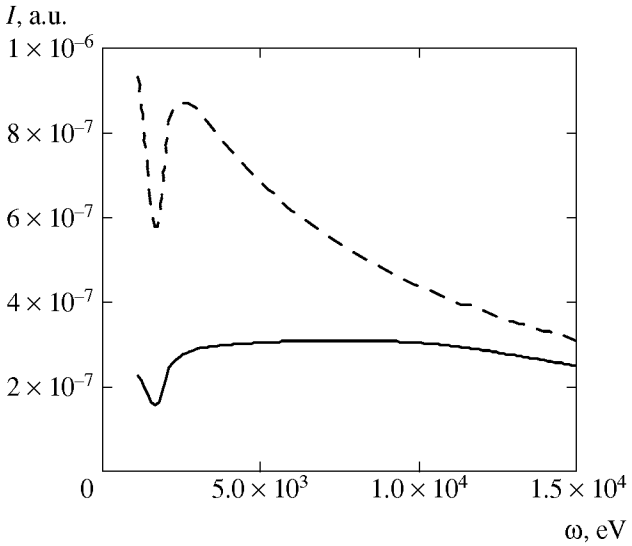

Fig. 2. Spectral PB intensity of an electron with $\gamma = 10$ on a silicon target at the emission angle $\theta = 18°$: PB in liquid silicon (solid curve) and on an isolated silicon atom (dashed curve).

destructive interference in PB. In the relativistic case, the minimum momentum transferred to the medium increases with emission angle and, as a result, the cooperative effects that produce the destructive interference decrease in importance. Therefore, the PB intensity for larger emission angles is suppressed at lower frequencies, when the minimum transferred momentum is fairly low and a few atoms of the medium are involved in the elementary radiative event.

In the low-frequency range ($\omega < 1$ keV), PB in liquid silicon was calculated for a relatively low incident electron energy ($\gamma = 3$) to exclude the Vavilov–Cherenkov effect, which can be significant [22], from our analysis. In this case, Cherenkov radiation takes place in a spectral range near the photoabsorption L edge of the silicon atom ($\omega \le 125$ eV). It follows from our calculations that the suppression effect in the low-frequency range reduces the PB intensity by almost an order of magnitude compared to the PB intensity on an isolated atom. Our analysis shows that the PB spectra in the case under consideration change only slightly when we pass to large emission angles. This is because the minimum momentum transferred to the medium depends weakly on the direction of photon emission with the parameters in question.

The angular dependence of the PB suppression ratio in an amorphous medium (13) is presented in Fig. 3. It shows the results of our calculations for an electron with a Lorentz factor of $\gamma = 100$ scattered in liquid silicon and two photon energies. We see that the angular range of the PB suppression effect narrows with increasing photon energy: $\theta < 100°$ for $\omega = 2720$ eV and $\theta < 40°$ for $\omega = 8160$ eV. Our analysis indicates that this angular narrowing increases with electron energy.

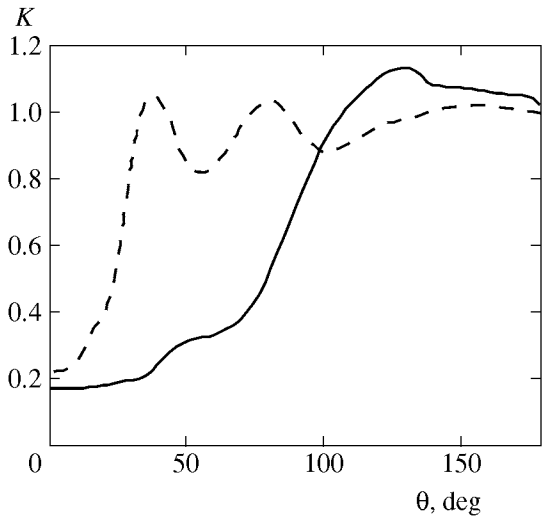

Fig. 3. Angular dependence of the PB suppression ratio for a relativistic electron ($\gamma = 10^2$) in liquid silicon for two bremsstrahlung photon energies: $\omega = 2720$ (solid curve) and 8160 eV (dashed curve).

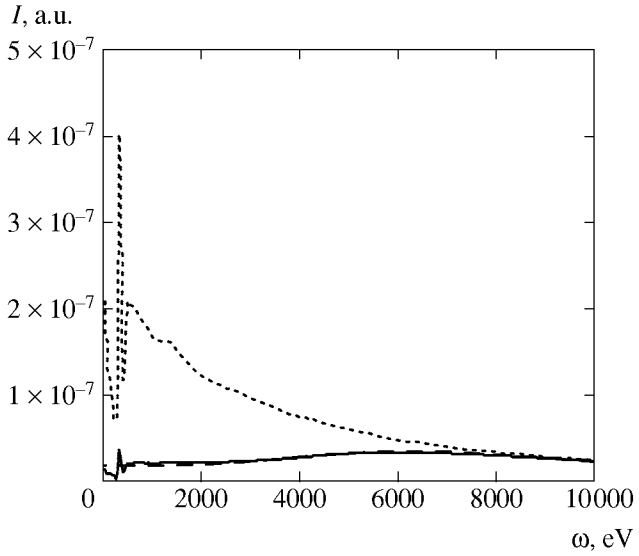

Fig. 4. Spectral PB intensity of a relativistic electron ($\gamma = 10$, $\theta = 45°$) on a carbon target: PB on a target of amorphous carbon (solid curve), on a carbon atom (dotted curve), and on amorphous carbon in the high-frequency approximation (dashed curve).

In contrast, in the nonrelativistic case, it is virtually absent. These trends are also determined by the dependence of the minimum transferred momentum (3) on the parameters of the problem.

As we noted in the Introduction, radiation from an electron with an energy of 5–7 MeV scattered by a thin-film target of amorphous carbon was detected in experiment [14], which demonstrated the PB suppression effect in an amorphous medium. Calculating the PB intensity for the experimental conditions [14] in the approach under consideration is of considerable interest. The corresponding results are shown in Fig. 4 for a Lorentz factor of the scattered electron of $\gamma = 10$, an emission angle of 45°, a target density of $\rho = 2.4$ g cm^{-3}, and a mean diameter of the carbon atom of $d = 1.258$ Å (at which $\sigma = 4\pi Nd^3/3 = 1$). The PB intensity in amorphous carbon calculated in the high-frequency approximation is also shown in this figure. It follows from the shapes of the curves that the suppression effect is most pronounced in the range of bremsstrahlung photon energies $\omega < 5$ keV, which corresponds to the experimental data from [14]. The maxima in the spectral dependences correspond to the binding energies of the electrons in the K and L shells of a carbon atom, 296 and 16.6 eV [20]. We also see that the high-frequency approximation describes well the process over a wide spectral range up to photon energies of 300 eV.

Our analysis shows that the error in the calculated PB intensity due to the inaccuracy of the model used for the structure factor of the medium depends on the parameters of the problem. This error is largest in the low-frequency range at large emission angles; in addition, it increases with incident electron energy. Comparison of the results of our calculations of PB in liquid silicon obtained in the hard-sphere model and using the quantum-chemical structure factor [17] gives a characteristic error of no more than 20% for $\gamma = 10$ and $\theta = 18°$. This error increases with emission angle, but the PB suppression effect itself decreases (Fig. 3).

In the case of a medium of heavy atoms, the structure factor can be calculated for the hard-sphere model (11) using tabulated values for the mean atomic diameter. This is because the atomic density of a material of heavy elements is relatively low and, hence, $\sigma < 1$. For example, for silver, $N = 5.85 \times 10^{21}$ cm^{-3}, $d = 2.88$ Å [18], and $\sigma = 0.583$. Our calculation of PB on a silver target shows that the PB suppression effect in the low-frequency range is considerably less pronounced than that on a target of amorphous carbon. Mathematically, this is attributable to the lower value of σ, which defines the structure factor of the medium in the hard-sphere model (11) used. Physically, the reduction in the PB suppression effect in low-density media can be explained by a decrease in the number of atoms in the formation region of an elementary radiative event and, accordingly, by a reduction in the importance of the destructive interference. In the range of high bremsstrahlung photon energies (at the same remaining parameters of the problem), the difference between PB on a silver target and the process on an isolated atom decreases and virtually vanishes for $\omega > 3$ keV. The difference between the results of using the two models of atomic polarizability (the high-frequency approximation and the consistent calculation) is very significant in the range $4.3 > \omega > 3.0$ keV, in which the L-subshell energies of the silver atom lie. In this range, the frequency dependence of the polarization charge is highly nonmonotonic.

The latter is reflected in Fig. 5, which presents the PB spectrum for an electron on a silver target in the high-frequency range for a larger incident electron energy, $\gamma = 10^3$, and a smaller emission angle, $\theta = 18°$. In this case, the suppression effect is more significant, particularly in the low-energy part of the spectrum. This is attributable to a lower minimum momentum transferred to the medium and, hence, to a clearer manifestation of the destructive interference between the contributions from various atoms of an amorphous medium to the amplitude of the polarization channel. Our calculation shows that the PB suppression effect for a relativistic particle in an amorphous medium becomes less pronounced as the emission angle increases. In addition, the spectral intensity maximum of the process is shifted toward the lower frequencies with increasing emission energy.

As we noted above, the minimum momentum transferred to the medium decreases with increasing incident particle energy; accordingly, the spatial PB formation region grows and the cooperative effects increase in importance. This is illustrated by Fig. 6, which shows the calculated dependences of the PB suppression ratio for an electron (13) in amorphous silver on the incident particle energy (more precisely, on $\gamma - 1$) for various photon energies and the emission angle $\theta = 18°$. Figure 6 also shows the straight line that corresponds to the PB suppression ratio obtained in the limit of low transferred momenta: $K = 1 - \sigma = 0.417$. As would be expected, the suppression effect is more pronounced for lower photon energies, when the destructive interference between the contributions from various atoms to the intensity of the process plays a great role. In the low-frequency range, PB is also suppressed for relativistic incident particles ($\gamma - 1 \ll 1$), while the PB intensity for high photon energies ($\omega > 1$ keV) decreases appreciably only in the case of large γ. A characteristic feature of the curves in Fig. 6 is the presence of such inflection points γ^* that the PB suppression begins for $\gamma > \gamma^*$. Note that the suppression ratio for large Lorentz factors, $\gamma > 10^4$, is smaller than its limiting value of $K = 1 - \sigma = 0.417$ (calculated with a logarithmic accuracy). This is attributable to the density effect in PB, when the intensity of the process decreases as a result of the screening of the intrinsic field of an incident particle at $\varepsilon(\omega) < 1$. The latter inequality for a silver target holds in the entire frequency range $\omega > 50$ eV of interest.

Similar dependences of the PB suppression ratio on the incident particle energy can be obtained for various emission angles and fixed bremsstrahlung photon energy. In this case, stronger PB suppression corresponds to smaller emission angles for the same reason as in the previous case.

A similar PB suppression effect in the low-frequency range takes place when a charged incident particle is scattered in a polycrystal [23, 24]. Just as in an amorphous medium, the interference between the contributions from atoms to the intensity of the polarization channel in a polycrystal for low transferred momenta, $q < 2\pi/a$ (a is the lattice constant), is destructive in nature, reducing the PB intensity. Note that an appreciable suppression ratio in an amorphous medium is possible only for relativistic incident particles (Fig. 6), while the PB intensity in a polycrystal decreases also significantly (by several factors) compared to an isolated atom in the nonrelativistic case [24].

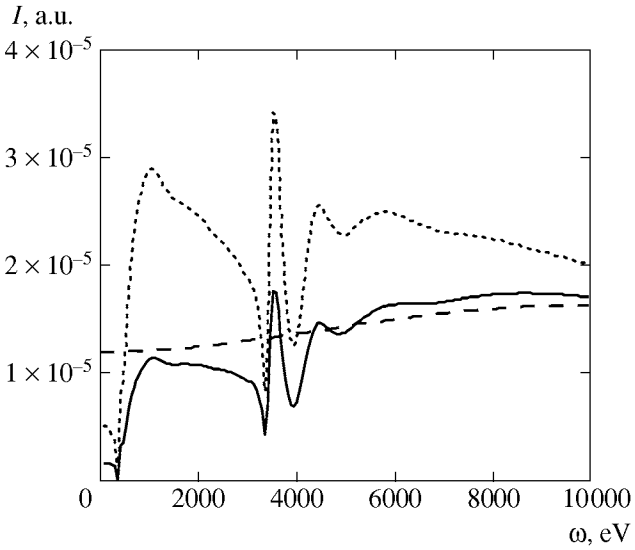

Fig. 5. Spectral PB intensity of a relativistic electron ($\gamma = 10^3$, $\theta = 18°$) on a silver target over a wide frequency range: PB on a target of amorphous silver (solid curve), on a silver atom (dotted curve), and on amorphous silver in the high-frequency approximation (dashed curve).

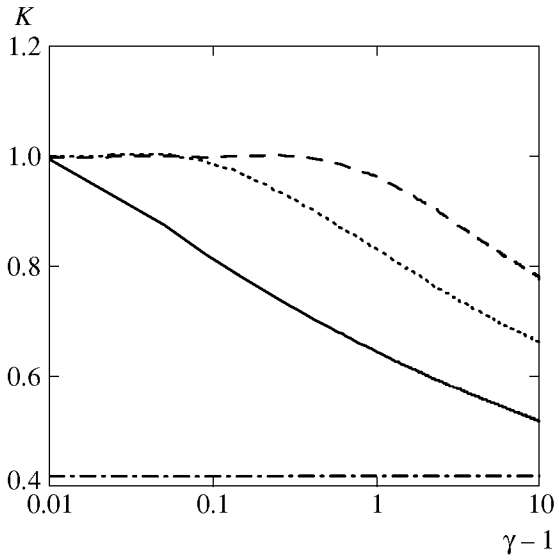

Fig. 6. PB suppression ratio in amorphous silver versus relativistic particle energy for the emission angle $\theta = 18°$ and three bremsstrahlung photon energies: $\omega = 300$ eV (solid curve), 1 keV (dotted curve), 3 keV (dashed curve), and $K = 1 - \sigma$ (dash–dotted line).

4. CONCLUSIONS

Our consistent quantum-mechanical calculation of the PB intensity showed that the suppression of the bremsstrahlung from a fast charged particle scattered in an amorphous medium plays an important role. The suppression effect results from the destructive interference between the contributions from various atoms of material chaotically arranged in the formation region of an elementary radiative event to the amplitude of the process. According to this physical picture, the more atoms of the medium are in the bremsstrahlung formation region, i.e., for low frequencies, high incident particle energies, and small emission angles, the more significant the PB suppression is. This conclusion is confirmed by our numerical analysis performed for several targets and various parameters of the problem.

The approach used to calculated the generalized atomic polarizability of the medium allowed PB to be investigated in the low-frequency range $\omega < 1$ keV, where the destructive interference is most significant and the PB suppression ratio is large. The PB suppression is shown to be at a maximum for materials composed of light atoms. For them, the dimensionless parameter $\sigma = 4\pi Nd^3/3$, which characterizes the atomic packing density, is close to unity. The angular dependence of the suppression ratio is most pronounced for relativistic incident particles and moderate photon energies, $1 < \omega < 10$ keV. At low frequencies $\omega < 1$ keV and for incident particles of relatively low energies ($\gamma - 1 \leq 1$), this dependence is weak.

We established the validity boundaries of the high-frequency approximation that was widely used in previous papers to calculate PB in a condensed material. This approximation was shown to be valid at $\omega >$ 100–200 eV for light atoms and at $\omega >$ 1–2 keV for heavy atoms.

The cooperative effect considered has its analog in PB on a polycrystal, where the PB intensity in the low-frequency range is considerably lower than its value on an isolated atom. The essential difference between the cooperative effects in PB on a polycrystal and the phenomenon considered here is that the constructive interference between the contributions from atoms of material to the bremsstrahlung amplitude causing an increase in the intensity of the polarization channel is also possible in the case of a polycrystal. This shows up particularly clearly for high-energy ($\gamma \gg 1$) charged particles in the frequency range in which the Bragg condition for the scattering of the virtual photon of the intrinsic field of an incident particle into a real photon is satisfied [23].

ACKNOWLEDGMENTS

This work was supported by the Ministry of Education and Science of Russia as part of the "Development of Scientific Potential of the Higher School" Program (project no. RNP.2.1.1.3263).

REFERENCES

1. *Polarized Bremsstrahlung from Particles and Atoms*, Ed. by V. N. Tsytovich and I. M. Oĭringel' (Nauka, Moscow, 1987) [in Russian].
2. V. A. Astapenko, L. A. Bureeva, and V. S. Lisitsa, Usp. Fiz. Nauk **172**, 155 (2002) [Phys. Usp. **45**, 149 (2002)].
3. A. V. Korol', A. G. Lyalin, and A. V. Solov'ev, *Polarization Bremsstrahlung* (S.-Peterb. Gos. Politekhn. Univ., St. Petersburg, 2004) [in Russian].
4. V. L. Ginzburg and I. M. Frank, Zh. Éksp. Teor. Fiz. **16**, 15 (1946).
5. Ya. B. Faĭnberg and N. A. Khizhnyak, Zh. Éksp. Teor. Fiz. **32**, 883 (1957) [Sov. Phys. JETP **5**, 720 (1957)].
6. M. L. Ter-Mikaelyan, *High Energy Electromagnetic Processes in Condensed Media* (Akad. Nauk Arm. SSR, Yerevan, 1969; Wiley, New York, 1972).
7. G. M. Garibyan and Yan Shi, Zh. Éksp. Teor. Fiz. **61**, 930 (1971) [Sov. Phys. JETP **34**, 1756 (1971)].
8. V. G. Baryshevskiĭ and I. D. Feranchuk, Zh. Éksp. Teor. Fiz. **61**, 941 (1971) [Sov. Phys. JETP **34**, 502 (1971)].
9. N. N. Nasonov and A. G. Safronov, in *Proceedings of International Symposium on Radiation of Relativistic Electrons in Periodic Structures* (Tomsk. Politekh. Univ., Tomsk, 1993).
10. S. Blazhevich, A. Chepurnov, V. Grishin, et al., Phys. Lett. A **254**, 230 (1999).
11. Y. Takabayashi, I. Endo, K. Ueda, et al., Nucl. Instrum. Methods Phys. Res. B **243**, 134 (2006).
12. R. W. James, *The Optical Principles of the Diffraction of X-rays* (Bell, London, 1962; Inostrannaya Literatura, Moscow, 1950).
13. N. N. Nasonov and A. G. Safronov, Zh. Tekh. Fiz. **62** (10), 1 (1992) [Sov. Phys. Tech. Phys. **37**, 973 (1992)].
14. S. V. Blaschevich, A. S. Chepurnov, V. K. Grishin, et al., Phys. Lett. A **211**, 309 (1996).
15. V. A. Astapenko, Zh. Éksp. Teor. Fiz. **128**, 88 (2005) [JETP **101**, 73 (2005)].
16. V. Ginzburg and V. Tsytovich, Phys. Rep. **49**, 1 (1979).
17. F. H. Stillinger and T. A. Weber, Phys. Rev. B **31**, 5262 (1985).
18. *Handbook on Physical Constants*, Ed. by I. S. Grigor'ev and E. Z. Meĭlikhov (Énergoatomizdat, Moscow, 1991; CRC Press, Boca Raton, 1997).
19. http://physics.nist.gov/PhysRefData/.
20. A. A. Radtsig and B. M. Smirnov, *Reference Data on Atoms, Molecules, and Ions*, 2nd ed. (Énergoatomizdat, Moscow, 1986; Springer, Berlin, 1985).
21. V. P. Shevelko, I. Yu. Tolstikhina, and Th. Stolker, Nucl. Instrum. Methods Phys. Res. B **184**, 295 (2001).
22. K. Yu. Platonov and I. N. Toptygin, Zh. Éksp. Teor. Fiz. **98**, 89 (1990) [Sov. Phys. JETP **71**, 48 (1990)].
23. N. N. Nasonov, Nucl. Instrum. Methods Phys. Res. B **145**, 19 (1998).
24. V. A. Astapenko, Zh. Éksp. Teor. Fiz. **126**, 1101 (2004) [JETP **99**, 958 (2004)].